ISSN 1392–1320 MATERIALS SCIENCE (MEDŽIAGOTYRA). Vol. XX, No. X. 2023

Blue/NIR-emitting Phosphor Based on Sr_2CeO_4: Tm^{3+}, Yb^{3+} Obtained by Combustion Synthesis

Nelson OSHOGWUE ETAFO [1], Joshua Omar CARRANZA [2], Carlos Eduardo RODRIGUEZ GARCIA [1, 2 *], Jorge OLIVA [3], Efrain VIESCA-VILLANUEVA [4], Ernesto HERNÁNDEZ-HERNÁNDEZ [5], Alejandro SANTIBAÑEZ [5], Oscar GOMEZ-ZAVALA [2]

[1] *Programa de Posgrado en Ciencia y Tecnología de Materiales, Facultad de Ciencias Químicas, Universidad Autónoma de Coahuila, Ing. J. Cárdenas Valdez S/N Republica, 25280 Saltillo, Coahuila*
[2] *Facultad de Ciencias Físico Matemáticas, Universidad Autónoma de Coahuila, Edif. A. S/N, unidad Camporredondo, CP 25000, Saltillo Coahuila. México*
[3] *CONACYT-Instituto Potosino de Ciencia y Tecnología Camino a la Presa de San José 2055, Lomas 4ta Secc., 78216 San Luis, S.L.P.*
[4] *Facultad de Ciencias Químicas, Universidad Autónoma de Coahuila, Ing. J. Cárdenas Valdez S/N Republica, 25280 Saltillo, Coahuila*
[5] *Centro de Investigación en Química Aplicada, Blvd. Enrique Reyna 140, Saltillo, Coahuila, 25253, México*

crossref http://dx.doi.org/10.5755/j02.ms.32518

Received 17 October 2022; accepted 06 January 2023

In this study, pure Sr_2CeO_4 (SCO) and codoped Sr_2CeO_4:Tm^{3+}, Yb^{3+} (SCO:Tm, Yb) of powder phosphors were synthesized by a combustion technique. The concentration of Tm^{3+} was fixed at 0.5 mol %, while the Yb^{3+} doping concentration was varied from 0 to 7.0 mol %. The crystalline structure, morphology and luminescence properties were studied using X-ray diffraction (XRD), scanning electron microscope (SEM) and photoluminescence spectroscopy, respectively. The XRD analysis shows the crystalline orthorhombic phase for all synthesized samples of SCO and SCO: Tm, Yb. The SEM results show that the doped sample with 5.0 mol % Yb^{3+} has the lowest grain particle size of 1.92 μm. The SCO:Tm, Yb phosphors produce mainly blue and near infrared emission bands centered at 481 nm and 813 nm (under 980 nm, excitation) which corresponds respectively to $^1G_4 \rightarrow {}^3H_6$ and $^3H_4 \rightarrow {}^3H_6$ transitions of Tm^{3+}. In addition, the international commission on illumination CIE coordinates were calculated for all samples taking the range of 400 – 700 nm obtaining for the 5.0 mol % Tm^{3+} doped sample the coordinates: (x,y) = (0.0833, 0.1671) which match with pure blue color. Due to the strong blue and near infrared emissions, the SCO:Tm, Yb phosphors could be good candidates for use in biomarkers or lighting applications.

Keywords: combustion synthesis, ytterbium, thulium, Sr_2CeO_4, blue emission.

1. INTRODUCTION

The current research in white light-emitting diodes (WLEDs) has increased in the last few decades because of their unique features such as environmentally friendliness, good fidelity, rapid response, good color coordination, short decay time, etc. [1]. Despite these advantages, a few limitations hinder the commercialization of phosphors on a large scale which include affecting the biological clock, irregularity of luminance and stronger re-absorption and the effect of blue light causing diseases like cataract, dry eye, and other age-related macular degeneration [2, 3].

An alternative Sr_2CeO_4 (SCO) blue phosphor was doped with Eu^{3+} to produce red and white emissions with high brightness [4]. Sr_2CeO_4 has an orthorhombic structure connected to one- dimensional chain of CeO_6 linked to Sr^{2+}.

The blue luminescence of SCO is due to the ligand to metal Ce^{4+} charge transfer and it has the following unique properties: 1) possesses a luminescent element that allows for spatial delocalization; 2) Efficient emission under ultraviolet, cathode ray and X-ray excitation; 3) thermal stability at temperature < 750 K 4) better optical properties because it occupies 4f level, the strong interaction of ceria and increased oxygen storage capacity [4 – 6].

There are previous reports of crystals such as Sr_2CeO_4:Er^{3+}, Yb^{3+}, Sr_2CeO_4:Eu^{3+}, La^{3+}, Sr_2CeO_4:Dy^{3+}, Li^+ and Sr_2CeO_4:Eu^{3+}, Sm^{3+} [7 – 10]. There have been no reports of any investigation of SCO co-doped with Tm^{3+} and Yb^{3+} obtained by combustion synthesis to the best of our knowledge.

The aim of this research is to produce blue emission under 980 nm excitation from Sr_2CeO_4 co-doped with Tm^{3+} and Yb^{3+} fixing the Tm^{3+} (0.5 mol %) and varied Yb^{3+} (0.5 – 7.0 mol %). The systematic structural, morphological, optical and photoluminescence properties investigation was carried out in detail, and we found blue/NIR-emitting phosphor of Sr_2CeO_4:Tm^{3+}, Yb^{3+} with upconversion mechanisms with 5.0 mol % of Yb co-doping as the best phosphor sample.

* Corresponding author. Tel.: +52-84-43-48-36-55.
E-mail address: *crodriguezgarcia@uadec.edu.mx* (C. R. Garcia)

2. EXPERIMENTAL

2.1. Synthesis of Sr_2CeO_4 and Sr_2CeO_4:Tm^{3+}, Yb^{3+} phosphors

The reagents thulium nitrate [$Tm(NO_3)_5 \cdot 5H_2O$, (99.99%)], ytterbium nitrate [$Yb(NO_3)_2 \cdot 5H_2O$, (99%)], strontium nitrate [$Sr(NO_3)$, (99.99%)], cerium nitrate [$Ce(NO_3)_3 \cdot 6H_2O$, (99.99%)], aluminum nitrate [$Al(NO_3)_3 \cdot 9H_2O$, (99.99%)] and urea [CH_4N_2O, (99.4%)] were acquired from Sigma Aldrich and used without further treatment.

The Sr_2CeO_4 (SCO) host and Sr_2CeO_4:Tm^{3+}, Yb^{3+} (SCO:Tm, Yb) phosphors were synthesized by using a combustion method using the following as shown in chemical Eq. 1:

$$2Sr(NO_3)_2 + (1 - x - y)Ce(NO_3)_3 \cdot 6(H_2O) + xTm(NO_3)_3 \cdot 5(H_2O) + yYb(NO_3)_3 \cdot 6(H_2O) + {}^{34}/_{6}\, NH_2CONH_2 \rightarrow Sr_2Ce_{(1-x-y)}O_4 + {}^{104}/_{6}\,(H_2O)\,(g) + {}^{55}/_{6}\,N_2(g) + {}^{34}/_{6}\,CO_2(g)\,. \quad (1)$$

The first sample was synthesized without any dopant and named SCO. The next five samples were synthesized using Yb concentrations of 0.5, 1.0, 1.5, 3.0, 5.0, 7.0 mol % with the constant Tm^{3+} co-doping concentration which was 0.5 mol % for all these SCO:Tm, Yb samples because the co-doping with the Tm, Yb in the other host matrix produces the highest upconversion emission according to the literature [11] and were named as SCO 0.5, SCO 1.0, SCO 1.5, SCO 3.0, SCO 5.0 and SCO 7.0 respectively.

The typical combustion synthesis of Yb and Tm co-doped SCO (sample SCO 1.0), $1.01 \cdot 10^{-2}$ mol of $Sr(NO_3)_2$, $7 \cdot 10^{-2}$ mol of $Ce(NO_3)_3$, $3.31 \cdot 10^{-5}$ mol of $Tm(NO_3)_3$ and $6 \cdot 10^{-6}$ mol of Yb $(NO_3)_3$ were mixed in 25 ml of distilled water in a beaker and stirred for 15 minutes and a transparent solution was formed. Then, 10 ml of an aqueous solution (urea 1M, $2.9 \cdot 10^{-2}$ mol) was slowly added for 5 minutes, and a viscous solution was obtained. Next, the beaker with the solution was put into a furnace previously heated at 600 °C and waited for 10 minutes, during this time the combustion process occurred.

As result, a yellow foam is formed and then subjected to grinding to obtain powders. Subsequently, the powders samples were subjected to an annealing treatment at 1100 °C for 6 hours in an air atmosphere using a heating rate of 10 °C/s.

2.2. Structural and morphological characterization

X-ray diffraction (XRD) characterization of the samples was obtained using a Panalytical Empyrean equipment with Cu-Kα radiation (λ = 1.5418 Å) in the range of $20° \leq 2\theta \leq 80°$ at a scan rate of 0.05 °/s.

The surface morphology of the SCO and SCO:Tm, Yb samples was visualized utilizing scanning electron microscopy by a Philips microscope Model XL30 operated at 30 kV. The average size of the microparticles of the different SCO Tm Yb were computed by employing the Image J software. The average of 10 microparticles of the SEM images of each representative sample was obtained carefully.

2.3. Optical and photoluminescence characterization

The photoluminescence (PL) spectra of the samples were collected with an Ocean optic Spectrometer USB 2000 coupled by a laser diode with excitation wavelength at 980 nm (200 mW of power) in the range 400 – 900 nm. All the PL measurements were performed under air conditions at room temperature (25 °C) and a NIR filter (900 nm cut off, IRC-09) was employed to eliminate the excitation wavelength from the emission spectra. The Chromaticity coordinates (CIE coordinates) were taken by using a Jenoptik CMOS camera under excitation at 980 nm.

3. RESULTS AND DISCUSSION

3.1. Structural and morphological studies of Sr_2CeO_4 and Sr_2CeO_4:Tm^{3+}, Yb^{3+} phosphors

The Sr_2CeO_4 host shows an orthorhombic structure with a space group Pbam (No 55) having lattice parameters a = 6.1189 Å, b = 10.3495 Å and c = 3.5970 Å [12]. The Diamond 3.1 software was used to carefully visualized and simulated the orthorhombic structure of Sr_2CeO_4 and presented in Fig. 1. The green, yellow, and red spheres represent Strontium, Cerium and Oxygen atoms respectively. The structure also showed polyhedrons of CeO_6 octahedra as an edge sharing linear chain and each Strontium atom is attached to four oxygen atoms as shown in light gray octahedra in a unit structure in Fig. 1.

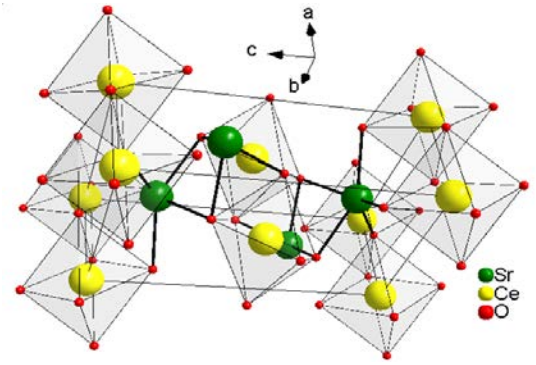

Fig. 1. Visualization of the crystalline structure of pure orthorhombic Sr_2CeO_4. The green, yellow, and red spheres corresponding to Sr, Ce, and O atoms, respectively

In the SCO:Tm^{3+}, Yb^{3+}, the ionic radiuses for the atoms are Sr^{3+} = 1.18 Å, Ce^{3+} = 0.87 Å, O^{2-} = 1.24 Å, Tm^{3+} = 1.134 Å and Yb^{3+} = 0.86 Å respectively [12]. Tm^{3+} has a lower ionic radius than Sr^{2+} thus making the substitution process easier but the Yb^{3+} dopant can easily be located into the Ce^{4+} site because their ionic radii are very close [12]. It has also been confirmed that Yb^{3+} can also be found in the Sr^{2+} site because it has an inter-chain site which produces charge imbalance with the Ce^{4+} site located at the center of the octahedra [12].

The XRD patterns for the undoped SCO and co-doped SCO:Tm, Yb for samples SCO 0.5 – SCO 7.0 are shown in Fig. 2 and all the reflected peaks were observed to match very well with the same diffraction peaks as the standard patterns of the pure Sr_2CeO_4 (JCPDS 50-0015 card), which corresponds to the orthorhombic crystalline phase diffracted peaks and no additional phase was observed [12].

The standard pattern is plotted in vertical lines at the bottom of the graph in Fig. 2. The orthorhombic crystalline phase is therefore maintained as the concentration of Yb increases as high as 7.0 mol %. The most intense diffraction peaks correspond to (130), (111) and (221) orientations at 2θ = 29.9º, 2θ = 30.4º and 2θ = 42.8º respectively which are labelled on the SCO 7.0 XRD pattern.

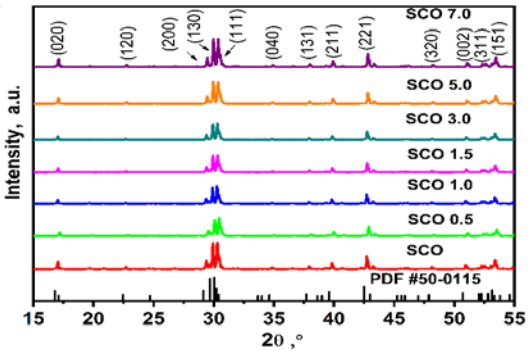

Fig. 2. X-ray diffraction patterns of Sr_2CeO_4 and various co-dopants concentrations: Yb = 0.5, 1.0, 1.5, 3.0, 5.0, 7.0 mol % and Tm = 0.5 mol % (fixed). SCO sample is without co-dopants

The a, b and c lattice parameters were calculated by using the diffraction peaks located at 2θ = 29.15º, 34.62º and 42.8º which corresponds to (200), (040) and (221) planes respectively to confirm the results.

The lattice parameters and the volume listed in Table 1 have reduced from 222.5 Å³ (SCO 0.5 sample) which is close to the reported in the literature of 227.62 Å³ [13] and slightly decreases to 221.03 Å³ (SCO 7.0 sample) which reveals that the lattice contraction of the crystalline structure network could be attributed to the Yb^{3+} and Tm^{3+} are lower in ionic radii than Sr^{2+} and Ce^{4+} respectively as reported by Viesca-Villanueva et al [14].

The crystallite size was calculated using the Scherrer equation [15] with the formula:

$$D = k\lambda/(\beta\cos\theta)\,, \qquad (2)$$

where k is the shape factor (0.9); λ is the wavelength (1.5418 Å); β is the full width at half maximum (FWHM); θ is the diffracted Bragg angle.

We calculated the crystallite mean sizes by using the XRD peak planes (020), (130) and (120). The crystallite mean sizes are listed in Table 1. The crystallite sizes ranging from 58.67 to 71.82 nm for the SCO – SCO 7.0 samples.

The SEM images show the morphology of the representative samples of SCO:Tm, Yb with the irregular shape at micro scale size. Fig. 3 a shows the micrograph of SCO 1.0, we detect coalesced particles with irregular shapes with the average size of 2.85 µm as is marked in a yellow circle. Fig. 3 b shows the micrograph SCO 3.0 sample, a lower irregular number of grains are observed with an average size of 2.44 µm (see blue circle).

If the concentration of Yb^{3+} is incremented to 5.0 mol %, a higher agglomeration degree among the microparticles is observed as is shown in the micrograph of SCO 5.0 presented in Fig. 3 c (see green circle), the average particle size decreases to 1.92 µm in this case. For the microparticles made with the Yb^{3+} concentration of 7.0 mol % (SCO 7.0 sample), a huge conglomeration of microparticles with a size of 2.04 µm are visualized in Fig. 3 d (see purple circle).

Table 1. The volume and crystallite size of the SCO phosphors co-doped at different concentrations: Co-dopants concentrations: Yb = 0.5, 1.0, 1.5, 3.0, 5.0, 7.0 mol % and Tm = 0.5 mol % (fixed). SCO sample is without co-dopants

Sample	a (Å)	b (Å)	c (Å)	Volume, Å³	Crystallite size, nm
SCO	6.068	10.277	3.567	222.504	70.98
SCO 0.5	6.064	10.244	3.585	222.722	58.67
SCO 1.0	6.079	10.286	3.565	222.978	69.70
SCO 1.5	6.073	10.289	3.528	220.505	71.82
SCO 3.0	6.073	10.270	3.553	221.290	71.65
SCO 5.0	6.063	10.270	3.553	221.290	65.92
SCO 7.0	6.058	10.267	3.553	221.032	66.24

In general, the SEM results agree with our previous studies that increasing the concentration of Yb^{3+} co-dopant increases the conglomeration among the SCO Tm, Yb microparticles [16]. This fact could create an imbalance of charges that causes a random growth of the microparticles with big sizes and irregular shapes because of the high content of Yb^{3+} [16].

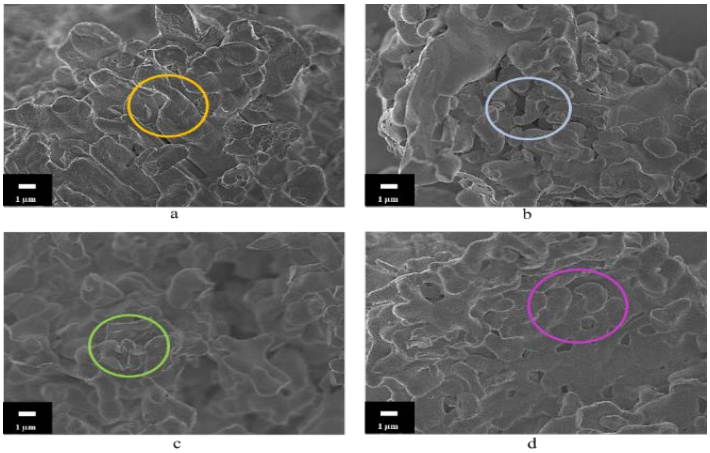

Fig. 3. SEM images for SCO:Tm, Yb samples, with Tm = 0.5 mol % fixed: a – SCO 1.0 (Yb = 1.0 mol %); b – SCO 3.0 (Yb = 3.0 mol %); c – SCO 5.0 (Yb = 5.0 mol %; d – SCO 7.0 (Yb = 7.0 mol %)

This decrement in grain sizes of SCO 5.0, has been reported in the literature for other phosphors that enhance the photoluminescence intensity [14]. The texture coefficient $Tc_{(hkl)}$ [17] of the *hkl* planes for SCO, SCO 1.0, SCO 3.0, SCO 5.0 and SCO 7.0 samples were obtained from the measured intensity $I_{(hkl)}$ and the relative intensity $I_{o(hkl)}$ of the corresponding plane given in JCPDS 50-0015 standard card, also n is the number of diffraction peaks. The $Tc_{(hkl)}$ formula is:

$$T_{C(hkl)} = \frac{I(hkl)/I_o(hkl)}{\frac{1}{n}\sum\frac{I(hkl)}{I_o(hkl)}}. \quad (2)$$

We calculated the T_C by using the XRD peak planes (111), (130) and (120). The texture coefficient values are listed in Table 2. We observe in general that the *Tc* increase for all the planes, and for the (130) plane the SCO1.0 sample has the highest value T_C = 1.131 that can be attributed to an increase in grains coalescence as reported elsewhere [17].

Table 2. Texture coefficient values calculated by using the XRD peak planes (111), (130) and (120)

Sample/ $T_{C\,(Plane)}$	$T_{C\,(111)}$	$T_{C\,(130)}$	$T_{C\,(120)}$
SCO	0.932	1.027	1.063
SCO 1.0	0.868	1.131	1.000
SCO 3.0	0.812	1.121	1.067
SCO 5.0	0.885	1.041	1.075
SCO 7.0	0.927	1.056	1.017

Considering the (120) diffracted plane, we observe an increase in the T_C from 1.000 to 1.075 for the SCO 1.0 and SCO 5.0 samples, respectively (as seen in Table 2), as well as in comparison with the other samples (SCO, SCO 3.0 – SCO 7.0). A highest value for the texture coefficient can be related to a better arrangement of atomic planes [18]. We inferred that the sample SCO 5.0 has the most pronounced texture ($T_{C\,(120)}$ = 1.075), which can be viewed as a more regular stacking, compared with SCO 1.0 for which the texture coefficient is smaller ($T_{C\,(120)}$ = 1.000), this could be beneficial for an enhancement on photoluminescence properties [18].

3.2. Luminescence of Sr_2CeO_4: Tm^{3+}, Yb^{3+} phosphors

Fig. 4 a – c shows the PL upconversion emission spectra of all the prepared samples in the range of 400 to 900 nm which were excited at 980 nm. Four main emission peaks can be detected and the highest are located at 813 and 795 nm that are linked to $^3H_4 \rightarrow {}^3H_6$ transition of Tm^{3+}, followed by emission at 481 nm which corresponds to $^1G_4 \rightarrow {}^3H_6$ and the least emission at 656 nm link to $^1G_4 \rightarrow {}^3F_4$ which confirms the reports in the literature [19, 23 – 25].

Fig. 4 b show an amplification of PL spectra showing the 481 nm peak from Tm^{3+} that is enhanced by the sensitizer Yb^{3+} under 980 nm excitation has been observed in different hosts [21, 22 – 24]. Also, Fig. 4 c presents the high-resolution PL spectra in the range of 720 – 860 nm.

We observed further that as the concentration increases in the SCO:Tm, Yb both the visible and NIR emissions are enhanced until a maximum value of 5.0 mol %. At a higher concentration of Yb, the emission was observed to be quenched due to quenching concentration (found in a similar system like $BaLaAlO_4$: Yb^{3+}, Tm^{3+} co-doped up to 7.0 mol % Yb) [24].

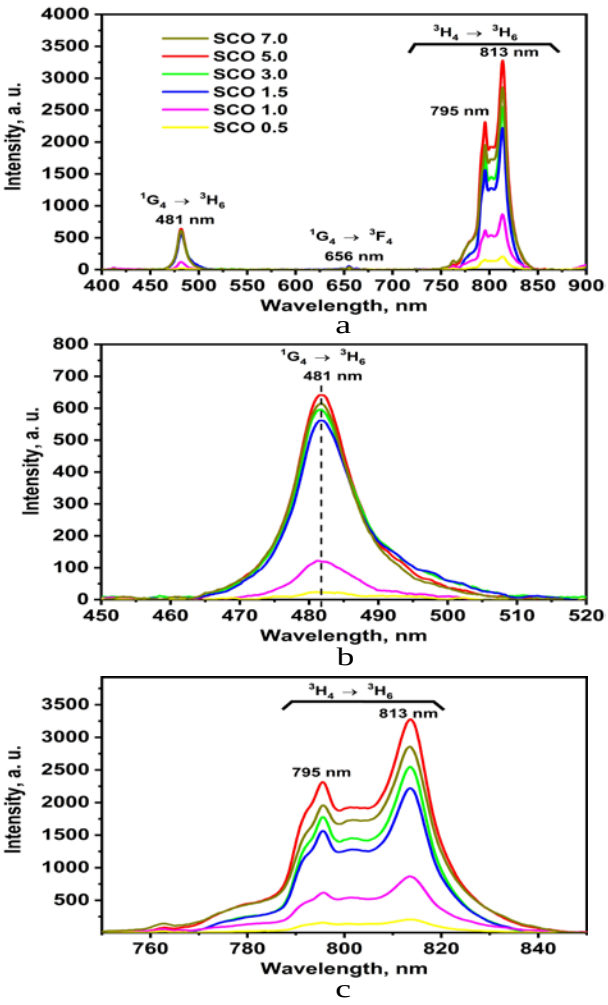

Fig. 4. a – PL emission spectra of SCO:Tm, Yb samples under 980 nm excitation; b – PL high resolution spectra of the range 450 – 520 nm; c – PL high resolution spectra in the range of 720 – 860 nm. Co-dopants concentrations: Yb = 0.5, 1.0, 1.5, 3.0, 5.0, 7.0 mol % and Tm = 0.5 mol % (fixed) for all samples

Thereafter, the contribution of the diverse emission to the overall emission was calculated. For 0.5 – 1.5 mol % Yb, represents blue emission 3 – 12 % of the overall visible emission in the SCO:Tm, Yb phosphors. For 1 – 5 mol % Yb, the maximum contribution of the red emission is 0.64 % while the NIR emission is the main component (88.3 – 93.6 %) of the overall emission in all the samples. The 813 nm Tm^{3+}emission co-doped with Yb^{3+}has been reported of having potential applications in vitro and in vivo bioimaging [26].

The Commission International de I' Eclairage (CIE) Chromaticity of Sr_2CeO_4 co-doped with Tm^{3+} and Yb^{3+} was discovered from the PL spectra at 980 nm laser excitation wavelength. Fig. 5 shows the CIE 1931 chromaticity diagram excited at 980 nm.

The color coordinates of Sr_2CeO_4: Tm^{3+}, Yb^{3+} for SCO 1.0 – 7.0 mol.% are plotted in Fig. 5. The photograph was taken using an IR filter in the darkness, we observed at 481 nm that the CIE color coordinates to produce a bluish-white emission, and this is confirmed with the color

coordinates present in the bluish-white region of CIE chromaticity diagram (and as shown by an inset shows the enlarged phosphors sample). The inset in Fig. 5 shows the photograph of SCO 5.0 sample as the most intense emission under excitation of 980 nm.

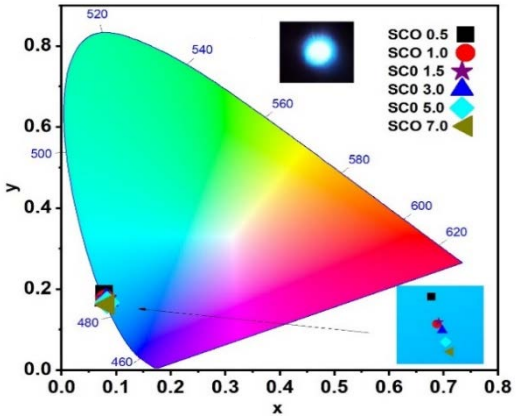

Fig. 5. The CIE map showing the color coordinates of SCO:Tm, Yb samples. As an inset a photograph of the SCO 5.0 sample under IR (980 nm) excitation is presented. At the right-bottom we show a magnification of the color coordinates which tend to be more pure blue as Yb increased. Co-dopants concentrations: Yb = 0.5, 1.0, 1.5, 3.0, 5.0, 7.0 mol % and Tm = 0.5 mol % (fixed) for all samples

Fig. 6 shows the energy level diagram excited at 980 nm. Yb^{3+} ion is excited from the ground state to the excited energy level, $^2F_{5/2}$.

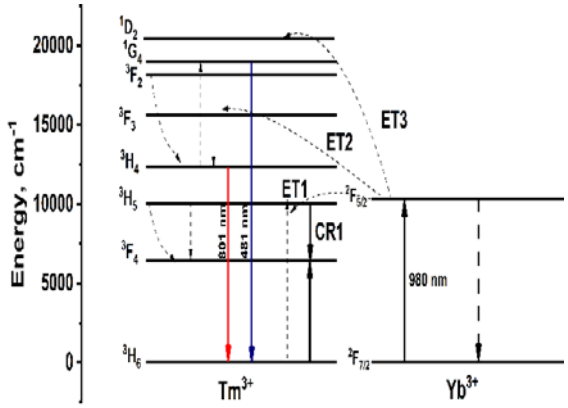

Fig. 6. Proposed energy diagram for SCO:Tm, Yb

This leads to the first energy transfer (ET1) which causes Yb^{3+} to move towards the Tm^{3+} and will also populate the $^3H_5$ level of Tm^{3+} from $^3H_6$ ground state. Thereafter, the electrons of the $^3H_5$ level are relaxed by multiphononic transitions to the $^3F_4$ level. From this level, a second photon was absorbed by the radiative relaxation of another Yb^{3+} ion (ET2) to excited to the $^3F_2$ level. From the $^3F_2$ level, it leads to a population of electrons by non-radiative relaxation again to the $^3H_4$ level and a third photon was absorbed at this level to become populated at the $^1G_4$ excited state (ET3). The electrons are then radiatively relaxed from $^3H_4$ and $^1G_4$ levels to the $^3H_6$ to produce the blue and NIR emission at 481 nm and 801 nm respectively [16].

4. CONCLUSIONS

In this study, the luminescent powders of SCO:Tm^{3+}, Yb^{3+} were successfully fabricated by the solution combustion synthesis. This was followed by thermal treatment at 1100 ℃ for 6 h. According to the XRD patterns, the orthorhombic phase was detected in all phosphors doped at (0.5 – 7.0 mol %) concentrations of Yb^{3+} and the pure one sample.

The SEM analysis confirms the key role of Yb^{3+} co-dopants in affecting the degree of coalescence of SCO Tm Yb phosphors and the intensity of photoluminescence with the lowest particle size was observed to be 5.0 mol % Yb^{3+}. The SCO:Tm^{3+}, Yb^{3+} was excited at 980 nm (at low optical power of 200 mW), the dominant NIR emission (813 nm) followed by the blue (481 nm) and the highest upconversion was observed to be 5.0 mol % Yb^{3+} followed by quenching at 7.0 mol % Yb^{3+}. The SCO:Tm, Yb could have a special interest in biomedical applications such as imaging probes, bioimaging and biosensors.

Acknowledgments

N.O. Etafo acknowledges to CONACYT-Mexico for the Ph.D. scholarship 1110994. C. R. Garcia acknowledges to DIP-UAdeC to support this investigation. We are greateful for the support from Laboratorio Nacional en Innovación y Desarrollo de Materiales Ligeros para la Industria Automotriz (LANIAUTO) No. 321156 and Laboratorio Nacional de Materiales Grafenicos (LNMG) No. 321244.

REFERENCES

1. **Ye, S., Xiao, F., Pan, Y.X., Ma, Y.Y., Zhang, Q.Y.** Phosphors in Phosphor-Converted White Light-Emitting Diodes: Recent Advances in Materials, Techniques, and Properties *Materials Science and Engineering: Reports* 71 (1) 2010: pp. 1 – 34. https://doi.org/10.1016/j.mser.2010.07.001
2. **Cho, J., Park, J.H., Kim, J.K., Schubert, E.F.** White Light-Emitting Diodes: History, Progress, and Future *Laser Photonics Review* 2017: pp. 16007. https://doi.org/10.1002/lpor.201600147
3. **Hargunani, S.P., Sonekar, R.P., Palaspagar, R.S., Patil, P., Omanwar, S.K.** Blue Luminescent Phosphor $Sr_3Y_{1-x}(BO_3)_3$:x Bi^{3+} for WLED Applications *Macromolecular Symposia* 387 (1) 2019: pp. 180018 1 – 5. https://doi.org/10.1002/masy.201800184
4. **Gupta, S.K, Sahu, M., Krishnan, K., Saxena, M.K., Natarajan, V., Godhole, S.V.** Bluish White Emitting Sr_2CeO_4: Eu^{3+} Nanoparticles Optimization of Synthesis Parameters, Characterization, Energy Transfer and Photoluminescence *Journal of Material Chemistry C* 1 (42) 2013: pp. 7054. https://doi.org/10.1039/C3TC31219D
5. **Ukare, R.S., Dubey, V., Zade, G.D., Dhoble, S.J.** PL Properties of Sr_2CeO_4 with Eu^{3+} and Dy^{3+} for Solid State Lighting Prepared by Precipitation Method *Journal of Fluorescence* 26 (3) 2016: pp. 791 – 806. https://doi.org/10.1007/s10895-016-1765-8
6. **Rao, C.A., Kumar, S.R., Murthy, K.V.R., Rao, B.S.** Effect of Flux on Sr_2CeO_4: Gd^{3+} (0.5 mol%) Phosphor Prepared by Solid State Reaction Method *International Journal of pure and applied physics* 14 (1) 2018: pp. 51 – 64.

https://www.ripublication.com/ijpap18/ijpapv14n1_07.pdf

7. **Seo, Y.W., Moon, B.K., Choi, B.C., Jeon, J.H., Choi, H., Kim, J.H.** Synthesis and Up-Conversion Luminescent Properties of Er^{3+}/Yb^{3+} Co-Doped Sr_2CeO_4 Phosphors *Ceramics International* 41 2015: pp 14332 – 14339. https://doi.org/10.1016/j.ceramint.2015.07.065
8. **Rao, C.A., Nannapaneni, P.R.V., Murthy, K.V.R.** Characterization and Photoluminescence of Sr_2CeO_4: Eu^{3+}, La^{3+} *Advanced Materials Letters* 4 2013: pp. 207 – 212. https://doi.org/10.5185/amlett.2012.7395
9. **Monika, D.L., Nagabhushana, H., Hari Krishna, R., Nagabhushana, B.M., Sharma, S.C., Thomas, T.** Synthesis and Photoluminescence Properties of a Novel Sr_2CeO_4: Dy^{3+} Nanophosphor with Enhanced Brightness by Li^+ Co-Doping *RSC Advances* 73 2014: pp. 38655 – 38622. https://doi.org/10.1039/C4RA04655B
10. **Jiao, H., Mao, C.L., Cai, R.** Photoluminescence of Red-Emitting Phosphor Sr_2CeO_4: Eu^{3+}, Sm^{3+} For Light Emitting Diodes *Advances in Computer Science Research* 76 2017: pp. 78 – 83. https://doi.org/10.2991/emim-17.2017.16
11. **Chen, D., Wang, Y., Bao, F., Yu, Y.** Broadband Near-Infrared Emission from Tm^{3+}/Er^{3+} Co-Doped Nanostructured Glass Ceramics *Journal of Applied Physics.* 101 2007: pp. 113511. https://doi.org/10.1063/1.2737395
12. **Danielson, E., Devenney, M., Giaquinta, D.M., Golden, J.H., Haushalter, R.C., McFarland, E.W., Poojary, D.M., Reaves, C.M., Weinberg, W.H., DiWu, X.** X-ray Powder Structure of Sr_2CeO_4: A New Luminescent Material Discovered by Combinatorial Chemistry *Journal of Molecular Structure* 470 (1 – 2) 1998: pp. 229 – 235. https://doi.org/10.1016/S0022-2860(98)00485-2
13. **Rao, C.A.O., Murthy, K.V.R.** Synthesis, Characterization and Luminescence Study of Erbium Doped Sr_2CeO_4 Nano Phosphor *International Journal of Scientific Development and Research* 5 2020: pp. 2455 – 2631.

    https://www.ijsdr.org/papers/IJSDR2004018.pdf
14. **Viesca-Villanueva, E., Oliva, J., Chávez, D., López-Badillo, C.M., Gómez-Solís, C., Mtz-Enriquez, A.I., García, C.R.** Effect of Yb^{3+} Codopant on the Upconversion and Thermoluminescent Emission of Sr_2CeO_4: Er^{3+}, Yb^{3+} Phosphors *Journal of Physics and Chemistry of Solids* 145 2020: pp 109547. https://doi.org/10.1016/j.jpcs.2020.109547
15. **Muniz, F.T.L., Miranda, M.A.R., Morrilla dos Santos, C., Sasaki, J.M.** The Scherrer Equation and the Dynamic Theory of X-ray Diffraction *Acta Crystallographica Section A Foundations and Advances* 72 2016: pp. 385 – 390. https://doi.org/10.1107/S205327331600365X
16. **Mu, Z., Hu, Y., Chen, L., Wang. X.** Enhanced Red Emission in Sr_2CeO_4: Eu^{3+} by Charge Compensation *Journal of The Electrochemical Society* 158 2011: pp. 287 – 235. https://doi.org/10.1149/1.3611678
17. **Consonni, V., Feuillet, G., Gergaud, P.** Plasticity Induced Texture Development in Thick Polycrystalline CdTe: Experiments and Modeling *Journal of Applied Physics* 103 2008: pp. 063529. https://doi.org/10.1063/1.2895382
18. **Romanitan, C., Tudose, I.V., Mouratis, K., Popescu, M.C., Pachiu, C., Couris, S., Koudoumas, E. Suchea, M.** Structural Investigations in Electrochromic Vanadium Pentoxide Thin Films *Physica Status Solidi A* 219 2022: pp. 2100431. https://doi.org/10.1002/pssa.202100431
19. **Pisarski, W.A., Pisarka, J., Lisiecki, R., Ryba-Romanowki, W.W.** Broadband Near-Infrared Luminescence in Lead Germanate Glass Triply Doped With $Yb^{3+}/Er^{3+}/Tm^{3+}$ *Materials* 14 2021: pp. 2901. https://doi.org/10.3390/ma14112901
20. **Ryba-Romanowski, W., Golvab, S., Sokolska, I., Dominiak Dizik, G., Zawadzka, J., Berkowski, M., Fink-Finowicki, J., Baba, M.** Spectroscopic Characterization of a Tm^{3+}: $SrGdGa_3O_7$ Crystal *Applied Physics B Lasers and Optics* 68 (2) 1999: pp. 199 – 205. https://doi.org/10.1007/s003400050606
21. **Jia, H., Xu, C., Wang, J., Chen, P., Liu, X., Qiu, J.** Synthesis of $NaYF_4$: Yb-Tm Thin Film with Strong NIR Photon Up-Conversion Photoluminescence Using Electro-Deposition Method *CrysEngComm* 16 (19) 2014: pp. 4023 – 4028. https://doi.org/10.1039/C4CE00078A
22. **Zhang, Y.Y., Wang, Y., Deng, J.Q., Wang, J., Ni, S.C.** Highly Efficient Yb^{3+}/Tm^{3+} Co-Doped $NaYF_4$ Nanotubes: Synthesis and Intense Ultraviolet to Infrared Up-Conversion luminescence *Optics Communications* 312 2014: pp. 43 – 46. https://doi.org/10.1016/j.optcom.2013.09.012
23. **Amorin, H.T., Vermelho, M.V.D., Gouveia-Neto, A.S., Casanjes, F.C., Ribeiro, S.J.L., Messaddeq, Y.** Red-Green-Blue Upconversion Emission and Energy-Transfer Between Tm^{3+} and Er^{3+} Ion in Tellurate Glasses at 1.064 μm *Journal of Solid State Chemistry* 171 2003: pp. 278 – 281. https://doi.org/10.1016/S0022-4596(02)00176-7
24. **Etafo, N.O., García, C.R., Oliva, J., Ruiz, J.I., Mtz-Enríquez, A., Avalos Belmonte, F., López-Badillo, C., Gómez-Solís, C.** Enhancing Blue/NIR Emission of Novel $BaLaAlO_4$:Yb^{3+} (x mol%) Tm^{3+}(0.5 mol%) Upconversion Phosphors with Yb^{3+} Concentration (x=0.5 to 6) *Inorganic Chemistry Communications* 137 2022: pp. 109192. https://doi.org/10.1016/j.inoche.2021.109192
25. **Bettencourt-Dias, A.D.** Luminescence of Lanthanide Ions in Coordination Compounds and Nanomaterials, John Wiley and Sons, Ltd. 1st Ed. 2014. https://doi.org/10.1002/9781118682760
26. **Zhao, P., He, K., Han, Y., Zhang, Z., Yu, M., Wang, H., Yao, S.** Near-Infrared Dual Emission Quantum Dots-Gold Nanoclusters Nanohybrid Via Co-Template Synthesis for Ratiometric Fluorescent Detection and Bioimaging of Ascorbic Acid in Vitro and in Vivo *Analytical Chemistry* 87 2015: pp 9998 – 10005. https://doi.org/10.1021/acs.analchem.5b02614